Poultry Science®

Inhibition of calcium imbalance protects hepatocytes from vanadium exposure-induced inflammation by mediating mitochondrial-associated endoplasmic reticulum membranes in ducks

Yiling Zhang,[*,†,1] Guyue Li,[*,1] Yanqing Zhao,[‡] Xueyan Dai,[*] Mingwen Hu,[*] Huabin Cao,[*] Kai Huang,[§] and Fan Yang[*,2]

[*]*Jiangxi Provincial Key Laboratory for Animal Health, Institute of Animal Population Health, College of Animal Science and Technology, Jiangxi Agricultural University, Nanchang 330045, China;* [†]*Department of Animal Science and Technology, Jiangxi Biotech Vocational College, Nanchang 330200, China;* [‡]*The Second People's Hospital, Jingdezhen 333099, China; and* [§]*Jiangxi Agricultural Engineering College, Zhangshu 331200, China*

ABSTRACT Vanadium (**V**) is an essential mineral element in animals, but excessive V can lead to many diseases, affecting the health of humans and animals. However, the molecular crosstalk between mitochondria-associated endoplasmic reticulum membranes (**MAMs**) and inflammation under V exposure is still at the exploratory stage. This study was conducted to determine the molecular crosstalk between MAMs and inflammation under V exposure in ducks. In this study, duck hepatocytes were treated with $NaVO_3$ (0 μM, 100 μM, and 200 μM) and 2-aminoethyl diphenyl borate (**2-APB**) (IP_3R inhibitor) alone or in combination for 24 h. The data showed that V exposure-induced cell vacuolization, enlarged intercellular space, and decreased density and viability. Meanwhile, hydrogen peroxide ($\mathbf{H_2O_2}$), malonaldehyde (**MDA**), catalase (**CAT**), superoxide dismutase (**SOD**), and reactive oxygen species (**ROS**) levels were upregulated under V treatment. In addition, excessive V could lead to a marked reduction in the MAMs structure, destruction of the membrane structure and overload of intracellular Ca^{2+} and mitochondrial Ca^{2+}. Moreover, V treatment resulted in notable upregulation of the levels of MAMs-relevant factors (IP_3R, Mfn2, Grp75, MCU, VDAC1) but downregulated the levels of IL-18, IL-1β, and lactate dehydrogenase (**LDH**) in the cell supernatant. Additionally, it also significantly elevated the levels of inflammation-relevant factors (NLRP3, ASC, caspase-1, MAVS, IL-18, IL-1β, and TXNIP). However, the inhibition of IP_3R expression attenuated the V-induced variations in the above indicators. Collectively, our results revealed that the maintenance of calcium homeostasis could protect duck hepatocytes from V-induced inflammation injury via MAMs.

Key words: vanadium, mitochondria-associated endoplasmic reticulum membrane, calcium homeostasis, inflammation, hepatocyte

2023 Poultry Science 102:103013
https://doi.org/10.1016/j.psj.2023.103013

INTRODUCTION

Vanadium (**V**) is an indispensable trace element that subsists the growth and development of organisms (Panchal et al., 2017; Janka, 2019). It has been widely used for industrial chemical catalysis, health care products, diabetes mellitus therapy, etc., due to its multifaceted biological roles (Harland and Harden-Williams, 1994; Tripathi et al., 2018). The mining, manufacturing, disposal of V, and associated products have caused serious environmental problems. Research has indicated that the average concentration of V in lake sediments is close to 95 mg/kg, which could present a risk for aquatic creatures and eventually enrich along the food chain, causing toxicity in humans (Zhou et al., 2019; Chetelat et al., 2021). V has been found to be mainly deposited in the liver and kidney due to the importance of these organs in detoxification of the organism and excretion of harmful substances (Scibior et al., 2020). Its inhalation induces liver damage, which activates inflammatory factors and the production of reactive oxygen species (**ROS**) (Han et al., 2021). It has been demonstrated that intraperitoneal exposure to sodium metavanadate induces an inflammatory storm and severe hepatotoxic damage (Adebiyi et al., 2018). Moreover, the over

© 2023 The Authors. Published by Elsevier Inc. on behalf of Poultry Science Association Inc. This is an open access article under the CC BY-NC-ND license (http://creativecommons.org/licenses/by-nc-nd/4.0/).

Received May 7, 2023.
Accepted August 4, 2023.

[1]The first 2 authors contributed equally to this work.

[2]Corresponding author: yfan2014001@163.com

addition of V to the diet of laying hens resulted in reduced albumen quality and antioxidant stress in the liver (Yuan et al., 2016). In summary, the liver is regarded as an important target involved in V poisoning due to its responsibility for metabolism and detoxification. The evidence shows that there are a large number of mitochondria and endoplasmic reticulum in the liver to adapt functions such as active biological oxidation. Hence, there is a strong possibility that the mitochondria and endoplasmic reticulum in the liver are the action sites of V. A previous study reported that chronic low doses of V exposure exacerbated mitochondrial deficits, increased ROS generation and influenced Ca^{2+} transport (Delfert and Mcdonald, 1985). Furthermore, our previous study suggested that excessive V could cause the dilatation and swelling of the ER, which induce ER stress and autophagy (Wang et al., 2022). It is proverbial that contact sites between the ER and mitochondria emerged mitochondrial-associated endoplasmic reticulum membranes (**MAMs**) as a crucial hub for various signaling pathways in the liver. However, the toxic effect of V on MAMs has rarely been discussed.

MAMs are the communication region between the ER and mitochondria, where various functional enzymes converge to cooperatively regulate cellular functions (Montesinos and Area-Gomez, 2020; Yang et al., 2020). Mitochondrial endoplasmic reticulum contacts are not only essential for organelle physiological functions and their mutual coordination, but also control intracellular lipid exchange, cell survival, and homeostasis in cellular metabolism (Yang et al., 2020). Importantly, MAMs are becoming an important hub involved in many fundamental cellular activities, such as apoptosis, Ca^{2+} signaling, and cellular inflammation (Barazzuol et al., 2021). Under abnormal conditions, changes in the distance and composition of MAMs lead to abnormal intracellular signal transduction, which will affect the physiological function of MAMs, such as altering Ca^{2+} homeostasis and leading to mitochondrial dysfunction. Ca^{2+} is a second messenger that is necessary for cellular homeostasis and plays a central role in numerous cellular functions (Park et al., 2020). The Ca^{2+} signal transduction pathway is a significant system constituted by the Ca^{2+} release channel protein IP_3R, porin VDAC1 and molecular chaperone GRP75, and it promotes MAMs differentiation and proliferation (Krols et al., 2016; Ahumada-Castro et al., 2021). The high expression of IP_3R is accompanied by the enhancement of interactions between the IP_3R-Grp75-VDAC1 complex and mitochondrial Ca^{2+} overload (Xu et al., 2018). A previous study showed that heavy metals could lead to mitochondrial impairment by inhibiting the regulation for the Ca^{2+} conduction pathway in the ER, and eventually lead to MAMs dysfunction (Peng et al., 2022). Studies have shown that Ca^{2+} is actively released and exerts an integral role in the management of the inflammatory reaction by stimulating mitochondria and ER during inflammation. However, the interaction mechanism between Ca^{2+} and MAMs in regulating inflammation is still unclear, especially in heavy metal-induced inflammation.

Indeed, MAMs provide a pivotal site for inflammasome formation, are attractive targets for heavy metals and are linked to Ca^{2+} channels (Bai et al., 2020). Inflammation is a rapid local supportive reaction to pathogenic microorganism influence and tissue damage, and almost all diseases are closely related to inflammation (Li et al., 2020). The NLRP3 inflammasome is a cytosolic multiprotein complex composed of the innate immune receptor protein NLRP3, adapter protein ASC, and inflammatory protease caspase-1 that responds to environmental stimuli, heavy metal poisoning and Ca^{2+} disorder (Dai et al., 2021). The NLRP3 inflammasome is a multiprotein signaling complex, that is, also assembled and activated in response to inflammation to catalyze the generation of the active forms of the potent proinflammatory cytokines IL-1β and IL-18. Research has confirmed that MAMs are molecular platforms required for active NLRP3 inflammasome formation where NLRP3 and its adapter ASC relocate to MAMs (Missiroli et al., 2018). Several studies have indicated that sodium metavanadate causes mitochondrial rupture and oxidative stress in hepatocytes, triggering inflammation (Hosseini et al., 2013; Renu et al., 2021). The levels of Ca^{2+} signaling play a crucial role in the structure of MAMs and promote the activation of the NLRP3 inflammasome (Wang et al., 2020). Previous studies have demonstrated that mitochondrial Ca^{2+} overload induces inflammation by opening the mitochondrial permeability transition pore when Ca^{2+} translocation is hyperactive and continuous. MAMs contain number of regulatory proteins that ensure the appropriate function of MAMs by maintaining optimal distances between organelles and coordinating ER and mitochondrial Ca^{2+} transport proteins or channels (Marchi et al., 2017). Similarly, Ca^{2+} transport in the ER of cells exposed to vanadate is inhibited, causing ER stress and promoting inflammation (Delfert and Mcdonald, 1985). However, there are few studies on whether V can trigger Ca^{2+} disorders and cellular inflammation via MAMs.

Our previous study showed that V could induce MAMs dysfunction and apoptosis in duck renal tubular epithelial cells. Based on our previous research on MAMs, we further explored whether MAMs could protect duck hepatocytes from V-induced inflammation injury and alleviate impaired liver function. Although MAMs have been confirmed to be significant in heavy metal studies, the interaction between the structural changes in MAMs under V exposure and the NLRP3 inflammasome is unclear. To determine the mechanism of MAMs in V-induced cell inflammation, 2-aminoethyl diphenyl borate (**2-APB**), an inhibitor of IP_3R, was used in this study to inhibit the activity of IP_3R (Slominski, 1991). Hence, in the current study, the duck hepatocyte model of V poisoning was applied to explore the mechanisms of MAMs in V-induced inflammation, which can better represent living tissues, are more vulnerable to cytotoxicity and have advantages over cell lines (Song et al., 2017).

MATERIALS AND METHODS

Cell Isolation and Cell Culture

Every animal experiment and procedure received approval from The Ethics Committee of The Agricultural University (Approval ID: JXAULL-2020-32). Briefly, the livers were removed from 13-day-old ducks, soaked in phosphate-buffered saline (**PBS**), stored on a plate and chopped. The tissue masses were then resuspended in Hank's balanced salt solution (**HBSS**) without Ca^{2+} and digested at 37°C for 15 min with 1 g/L collagenase (Sigma). Then Dulbecco's modified eagle medium (**DMEM**) (Gibco) containing 10% fetal bovine serum (**FBS**) was added, followed by centrifugation (200 × *g* for 5 min) twice (Yang et al., 2018). Finally, the hepatocytes were maintained in growth medium (**GM**), which consisted of insulin (0.57 μg/mL), streptomycin (80 U/mL), penicillin (80 U/mL), transferrin (5 μg/mL), dexamethasone (40 ng/mL), and L-glutamine (400 μg/mL). We constructed the models by treating with various concentrations of $NaVO_3$ (0, 25, 50, 100, 200, 400, and 800 μM) for 24 h and detected the half-maximal inhibitory concentration ($\mathbf{IC_{50}}$) values of V and the IC_{50} value was 228.20 μM (Figure S1) (0 μM V, 100 μM V, 200 μM V). Hepatocytes were treated with a range of 2-APB concentrations (MedChemExpress, Shanghai, China) (0, 5, 10, 20, 40 μM), and the most favorable concentration of 2-APB (10 μM) was confirmed (Figure S2). Thence, cells were grouped as follows: 0 μM V (control group), 200 μM V (V group), 200 μM V+ 2-APB (V+ 2-APB group), and 10 μM 2-APB (2-APB group).

Cell Viability Assay

Briefly, hepatocytes were seeded in 96-well plates at a density of 1 × 10^5/100 μL cells per well and incubated for 24 h; these were treated with V and/or 2-APB for 4 time periods. The plates were incubated for 2 to 3 h in a CO_2 incubator after the addition of CCK-8 as per the manufacturer's technical manual under dark conditions (Zhao et al., 2021). Finally, a microplate reader (ELX808; BioTek) was used to measure cell viability.

The Observation of Ultrastructure

Transmission electron microscopy (**TEM**) was applied for hepatocyte ultrastructural analysis after V and 2-APB exposure for 24 h, and the observation method was performed according to previous publications (Peng et al., 2022).

Immunofluorescence Staining

In brief, the hepatocytes were fixed in 4% buffered paraformaldehyde for 20 min. Afterward, hepatocytes were treated with the corresponding antibody. Mito-Tracker Green (Beyotime, Shanghai, China) and ER-Tracker Red (Beyotime, Shanghai, China) were used to calculate the number of fluorescent spots between mitochondria and the ER. Confocal fluorescence microscopy (Vutara352; Bruker, Germany) was applied to detect the fluorescence intensity (Miao et al., 2022).

Intracellular ROS Detection

In brief, 12-well plates were seeded with cells. After treatments, hepatocytes were dissociated with trypsin digestion for 4 min to obtain single hepatocytes. Then the hepatocytes were resuspended in GM, collected and separated from the solution using a centrifuge and washed twice. According to the ROS kit (Beyotime Biotechnology, Shanghai, China), the level of intracellular ROS was detected in a strict sequential order. Flow cytometry methods (C6 Plus BD) were used to evaluate cellular ROS levels after treatment (Fang et al., 2021).

Determination of IL-18, IL-1β, and LDH Levels

After V and 2-APB treatment, cell supernatants were analyzed to detect the IL-18, IL-1β, and LDH concentrations via kits (Mlbio, Nanjing, China; Nanjing Jiancheng Bioengineering Institute, Nanjing, China).

Determination of Oxidative Stress Indices

After digestion, washing and recollection, the levels of SOD, CAT, H_2O_2, and MDA were detected by commercial kits (Nanjing Jiancheng Bioengineering Institute, Nanjing, China) (Dai et al., 2022; Ea et al., 2022; Widowati et al., 2022). A microplate reader (ELX808; Bio-Tek) was used to calculate the absorbance at a certain wavelength.

Intracellular and Mitochondrial Ca^{2+} Level Detection

Intracellular and mitochondrial Ca^{2+} levels were measured with a Cell Permeant Kit (Fluo-4 AM, Rhod-2/AM) (Beyotime, Shanghai, China; Yeasen, Shanghai, China). The hepatocytes were incubated with Fluo-4 AM or Rhod-2 AM for half an hour at 37°C in the cell incubator. The levels of Ca^{2+} in the hepatocytes were measured by flow cytometry.

Quantitative Reverse Transcriptase-Polymerase Chain Reaction Analysis

The extraction method of total RNA was similar to a previous study (Wang et al., 2022). TRIzol reagent (Vazyme, Nanjing, China) was used to isolate the total RNA (0.05 g tissue per sample), and the purity and concentration of RNA were measured by a GeneQuant 1300 spectrophotometer. One microgram of total RNA was used to generate cDNA with an EasyScript One-Step gDNA Removal and cDNA Synthesis SuperMix Kit (Ea et al., 2022). Primer software was employed for PCR

Table 1. Gene name and their primer sequences.

Gene name	Primer sequences (50−30)
Mfn2	Forward: CTGGCATTGATGTAACCAC
	Reverse: CAAAGAAAATTCGATCCCCT
PACS-2	Forward: GATTGCCACCACTCCGACCA
	Reverse: TGCAAATCAACCTGCTGATGCC
Grp75	Forward: GTTCAAGAGAGAGACGGGCG
	Reverse: ATCAGATCAGCCACGATGCC
IP3R	Forward: TTCGCTAGGAGAGACCTGCT
	Reverse: CTCTGGCTTAGTGCCCCTTG
VDAC1	Forward: TGTTCCACCTGCTTATGCTG
	Reverse: AGCCTGTCTTAACTTTAGCG
MCU	Forward: CCATGAAAATGCAACTACGCTGA
	Reverse: TCCTCAATGCACAAGGCGGTA
Sig-1R	Forward: GGTGCTAAATGGCTGCATCG
	Reverse: TCTGGCGTCTTCCTAGCTCT
NLRP3	Forward: ATGTCCCGACTACCCTTCCA
	Reverse: GAGTAGTGTCTTCCGCACCC
ASC	Forward: CAGCATTCTGGATCGGCTCT
	Reverse: ATTTTCTCCTGCCTGATGCTT
MAVS	Forward: GATTCGTCTGGCACGTCTGA
	Reverse: TGGGTTTGGGGTTTGAGCTT
TXNIP	Forward: AAAGGTATTTTTGCCCGCCG
	Reverse: ATATGCCTTCTCAGGCTCGC
Caspase-1	Forward: GCAAATTCTTGCCAGGGAGC
	Reverse: GTCGGAGATCGTCACTGCTG
IL-18	Forward: GAGATGAAATCTGGCAGCGG
	Reverse: ACCCGGACACTGAATGCAAC
IL-1β	Forward: ACAAGCTCTACATGTCGTG
	Reverse: CAGGCGGTAGAAGATGAAG
β-actin	Forward: ATGTCGCCCTGGATTTCG
	Reverse: CACAGGACTCCATACCCAAGAAT

primer design (Table 1). Then, quantitative reverse transcriptase-polymerase chain reaction (**qRT-PCR**) was performed on a QuantStudio 7 Flex real-time PCR system (ABI 7900HT, Applied Biosystems). The mRNA levels of each gene were evaluated by the $2^{-\Delta\Delta CT}$ method, and the mRNA levels were normalized to β-actin maintenance gene levels (Xu et al., 2021).

Western Blotting

Western blotting was performed according to a previous study (Bai et al., 2021; Miao et al., 2022). Briefly, approximately 0.1 g of sample was homogenized in protein lysis solution. The obtained tissue homogenate was centrifuged to collect the supernatant, and its protein concentration was unified to the same concentration by the BCA method (Solarbio, Beijing, China). The processed protein samples were separated by gel electrophoresis and transferred to PVDF membranes (Bio-Rad). The primary antibodies were anti-IP_3R (1:800; Bioss, Beijing, China), anti-Mfn2 (1:800; Sigma), anti-Grp75 (1:500; Bioss, Beijing, China), anti-VDAC1 (1:1,000; Wanleibio, Shenyang, China), anti-NLRP3 (1:2,000; Wanleibio, Shenyang, China), anti-IL-18 (1:500; Wanleibio, Shenyang, China), anti-IL-1β (1:1,000; Wanleibio, Shenyang, China), anti-caspase-1 (1:500; Wanleibio, Shenyang, China), anti-ASC (1:500; Santa Cruz Biotechnology), and anti-GAPDH (1:3,000; Bioss, Beijing, China). Finally, ImageJ software was employed as an analytical method to analyze the related protein (Lin et al., 2023).

Statistical Analysis

The data were scrutinized and denoted as the mean ± standard deviation (**SD**) from at least 3 independent experiments. The statistical significance of the differences was determined using ANOVA. A P value of less than 0.05 was considered statistically significant. All statistical analyses were performed using SPSS 22.0, and GraphPad Prism 8.0 was used to analyze all statistics.

RESULTS

V Exposure-Induced Duck Hepatocyte Injury and MAMs Structural Abnormalities

The cell viability was significantly decreased ($P < 0.001$) with increasing exposure time and V concentration (Figure 1A). To explore whether V causes oxidative stress, we monitored the ROS level and antioxidant indicators. In Figure 1B and C, the intracellular ROS level was elevated after V treatment with time compared with the control group ($P < 0.05$, $P < 0.01$, or $P < 0.001$). As shown in Figure 1D to G, compared with the control group, the levels of MDA, SOD, H_2O_2, and CAT in the V-treated groups were markedly increased ($P < 0.05$, $P < 0.01$, or $P < 0.001$), and a dose effect was shown.

Morphological changes in MAMs were assessed, and the results are shown in Figure 1H and J. After V treatment, the number and length of MAMs decreased ($P < 0.01$ or $P < 0.001$), as observed by TEM. Meanwhile, after cells were treated with ER-Tracker and Mitotracker, the fluorescent spots of ER and mitochondria decreased, and the Pearson coefficient decreased noticeably ($P < 0.05$ or $P < 0.001$) (Figure 1I and K).

V Disturbed the Levels of MAMs-Related Factors by Affecting Calcium Homeostasis

The results showed that intracellular and mitochondrial Ca^{2+} levels were markedly increased ($P < 0.01$ or $P < 0.001$) after V treatment for 24 h (Figure 2A and B). With increasing of V concentration, the mRNA levels of IP_3R, Grp75, VDAC1, MCU, and MFN2 were remarkably higher than those in the control group (Figure 2C and D) ($P < 0.05$, $P < 0.01$, or $P < 0.001$). The protein levels of IP_3R, Mfn2, Grp75, and VDAC1 were also significantly upregulated ($P < 0.001$) (Figure 2E and F).

V Exposure-Induced Inflammation in Duck Hepatocytes

Compared with the control group, the contents of IL-18 and IL-1β were significantly increased under V exposure ($P < 0.001$) (Figure 3A). LDH levels increased significantly with increasing V concentrations ($P < 0.05$, $P < 0.01$, or $P < 0.001$) (Figure 3B). Figure 3C and D shows that the fluorescence intensity of NLRP3 and ASC was enhanced under V treatment. The

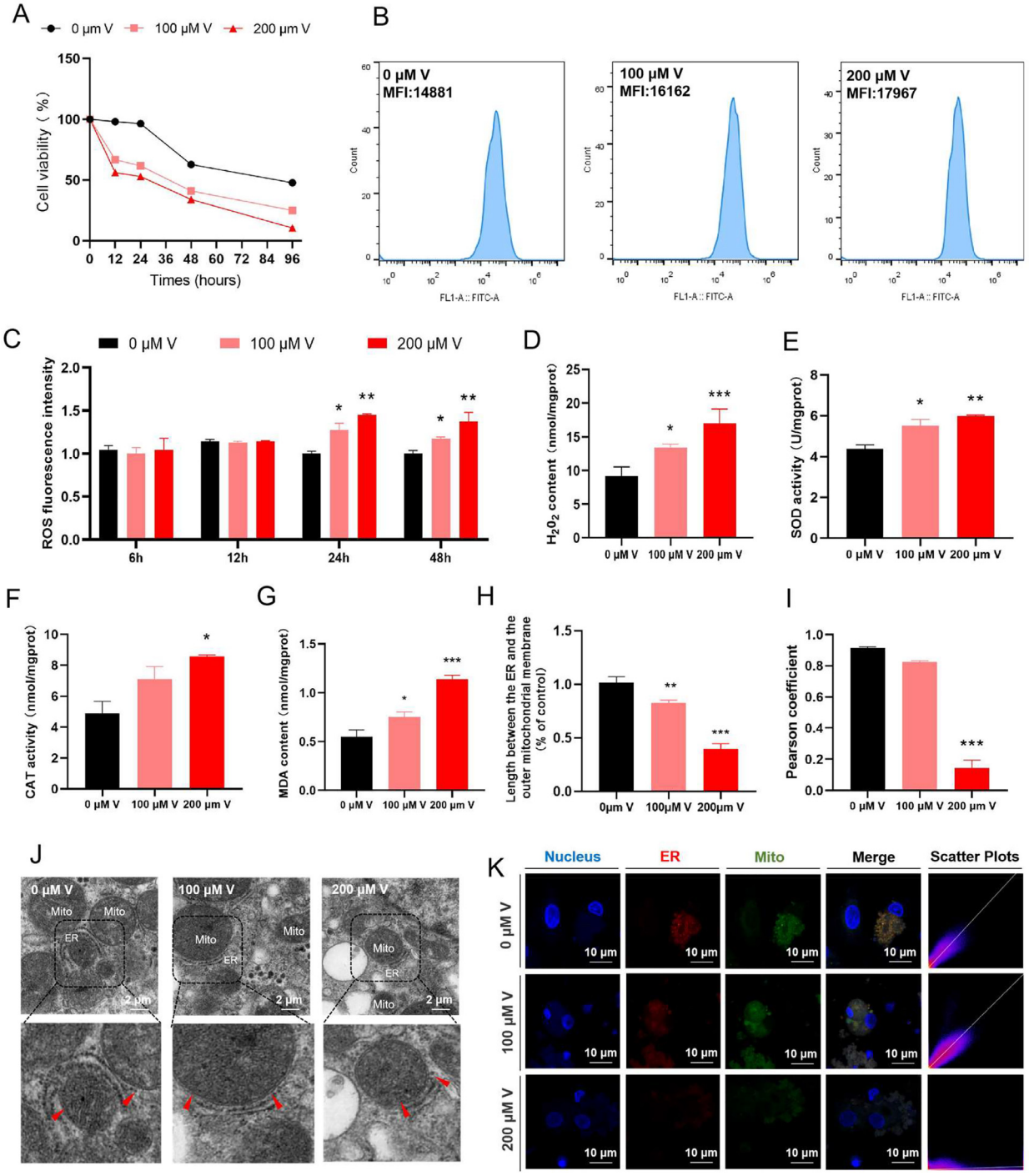

Figure 1. V exposure-induced duck hepatocyte injury and MAM structural abnormalities. (A) Changes in cell viability at 12, 24, 48, and 96 h. (B) ROS production at 24 h. (C) ROS levels at 6, 12, 24, and 48 h. (D–G) Oxidative stress indices. (H) Analysis of MAM length. (I) Pearson's coefficient analysis correlation of ER and Mito staining. (J) Ultrastructural observation. Mito: mitochondria; red arrows: ER-mitochondria coupling. (K) LSCM detection of ER and mitochondrial interactions (*$P < 0.05$ vs. Control, **$P < 0.01$ vs. Control, ***$P < 0.001$ vs. Control).

colocalization puncta of NLRP3 and ASC were increased significantly under V stress ($P < 0.01$ or $P < 0.001$).

The mRNA levels of NLRP3, ASC, caspase-1, MAVS, TXNIP, IL-18 and IL-1β also showed significant upregulation ($P < 0.01$ or $P < 0.001$) (Figure 3E and F). Compared with the control group, the protein levels of NLRP3, ASC, and caspase-1 were also significantly increased (Figure 3G and H) ($P < 0.05$ or $P < 0.001$).

2-APB Alleviated V-Induced Injury and MAMs Morphological Damage in Duck Hepatocytes

Compared with that of the V group, the cell viability of the V+2-APB group was notably increased ($P < 0.001$) (Figure 4A). Compared with the V group, the intracellular ROS level increased after V treatment ($P < 0.01$ or $P < 0.001$) over time (Figure 4B and C). Antioxidant indicators are shown in Figure 4D to G. Compared with the V group, the levels of MDA and SOD in the V

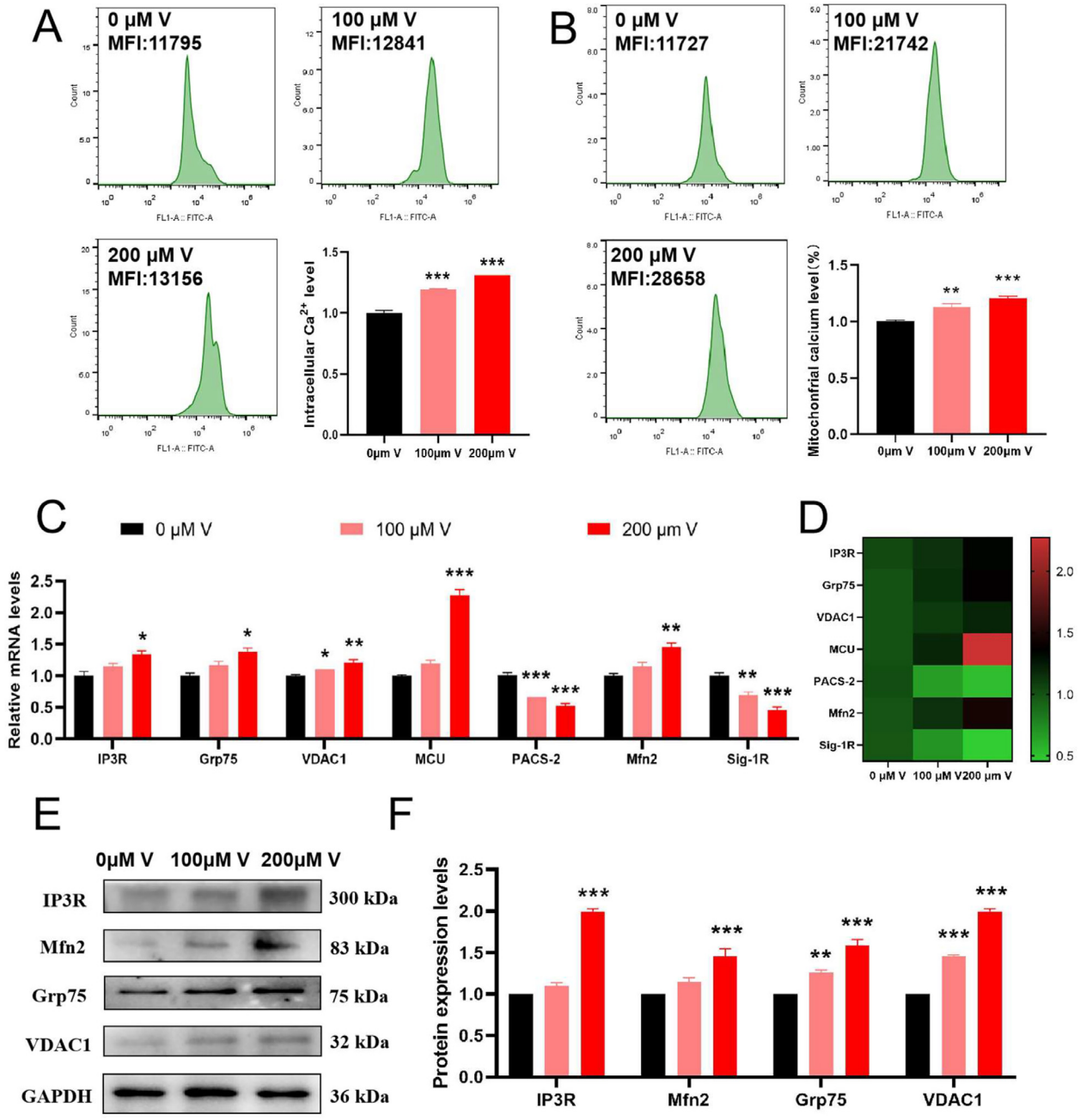

Figure 2. V disturbed the levels of MAM-related factors by affecting calcium homeostasis. (A) Intracellular Ca^{2+} level. (B) Mitochondrial Ca^{2+} level. (C and D) mRNA levels of MAM-related factors. (E and F) Protein levels of MAM-related factors (*$P < 0.05$ vs. Control, **$P < 0.01$ vs. Control, ***$P < 0.001$ vs. Control).

+2-APB group were greatly decreased ($P < 0.05$ or $P < 0.001$), and CAT and H_2O_2 tended to decrease (Figure 4D–G).

Morphological changes in MAMs were also evaluated, and the results are shown in Figure 4H and J. The structure of MAMs in the control group and 2-APB group was stable through TEM, while the number and length of MAMs in the V group were decreased enormously compared with the control group ($P < 0.001$). Compared with the V group, the number of fluorescent spots at the junction of the ER and mitochondria in the V+2-APB group tended to increase (Figure 4I and K).

2-APB Regulated V-Induced MAMs Dysfunction-Related mRNA and Protein Levels by Regulating Calcium Homeostasis

The experimental results showed that compared with the V group, the intracellular Ca^{2+} level in the V+2-APB group was considerably decreased ($P < 0.05$). In addition, the intracellular and mitochondrial Ca^{2+} levels were not significantly different in the 2-APB group compared with the control group (Figure 5A and B). qRT-PCR results showed that compared with the V group, the mRNA levels of IP_3R, Grp75, and MCU in the V+2-APB group were markedly

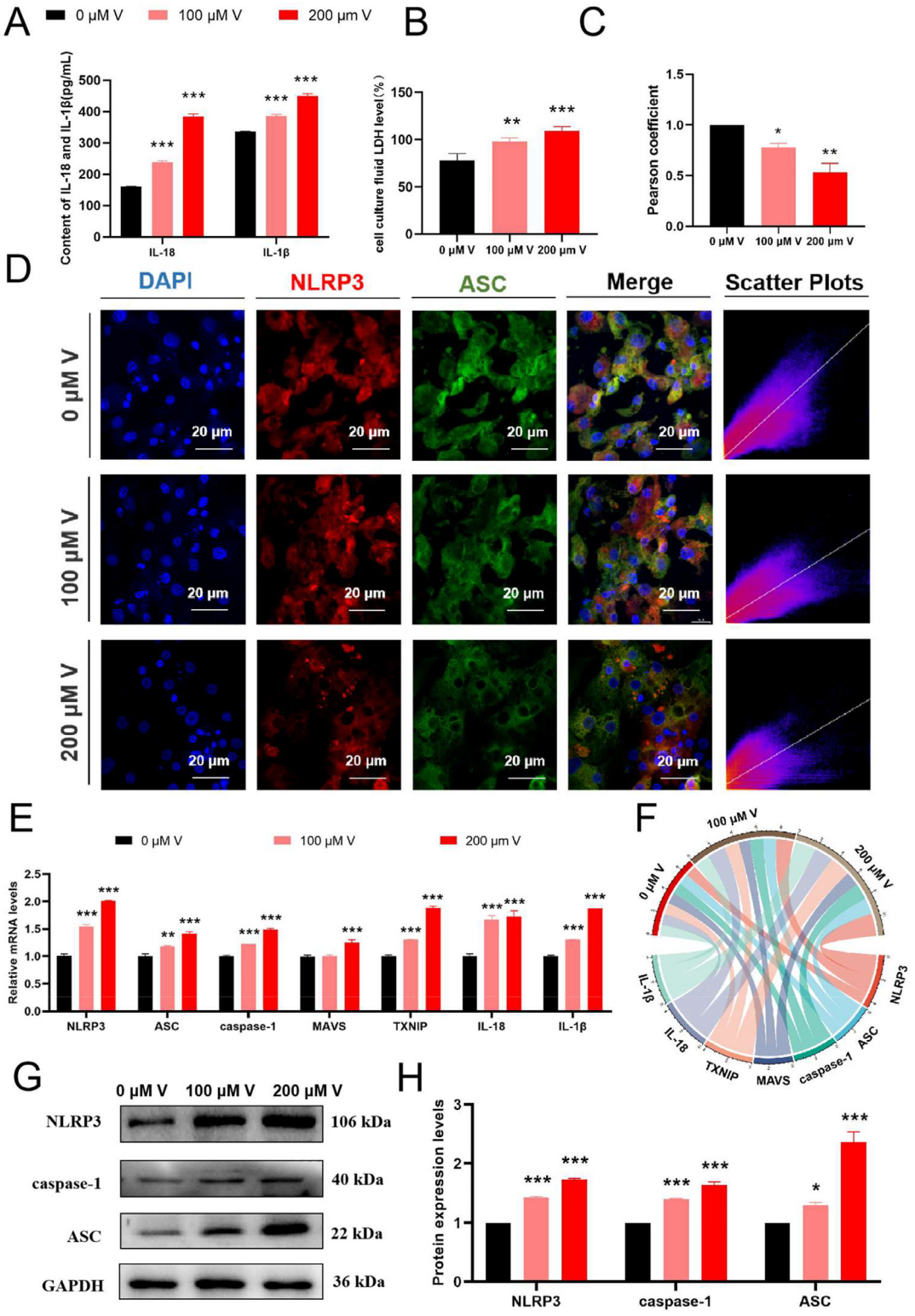

Figure 3. V-induced inflammation in duck hepatocytes. (A) IL-18 and IL-1β activities in the cell supernatant. (B) LDH activity in the cell supernatant. (C) The Pearson correlation coefficient of the colocalization of NLRP3 and ASC. (D) Observation of the colocalization of NLRP3 and ASC. (E and F) mRNA levels of inflammation-related factors. (G and H) Protein levels of inflammation-related factors (*$P < 0.05$ vs. Control, **$P < 0.01$ vs. Control, ***$P < 0.001$ vs. Control).

decreased ($P < 0.001$), and the mRNA levels of PACS-2 and Sig-1R were substantially increased ($P < 0.05$ or $P < 0.01$) (Figure 5C and D). The protein levels of IP_3R, Grp75, VDAC1, and Mfn2 were consistently steeply decreased ($P < 0.001$) (Figure 5E and F).

2-APB Reduced V-Induced Inflammation

Compared with the V group, the contents of IL-18, IL-1β, and LDH in the supernatant of the 2-APB group were significantly decreased ($P < 0.001$) (Figure 6A and B). Figure 6C and D shows that the fluorescence

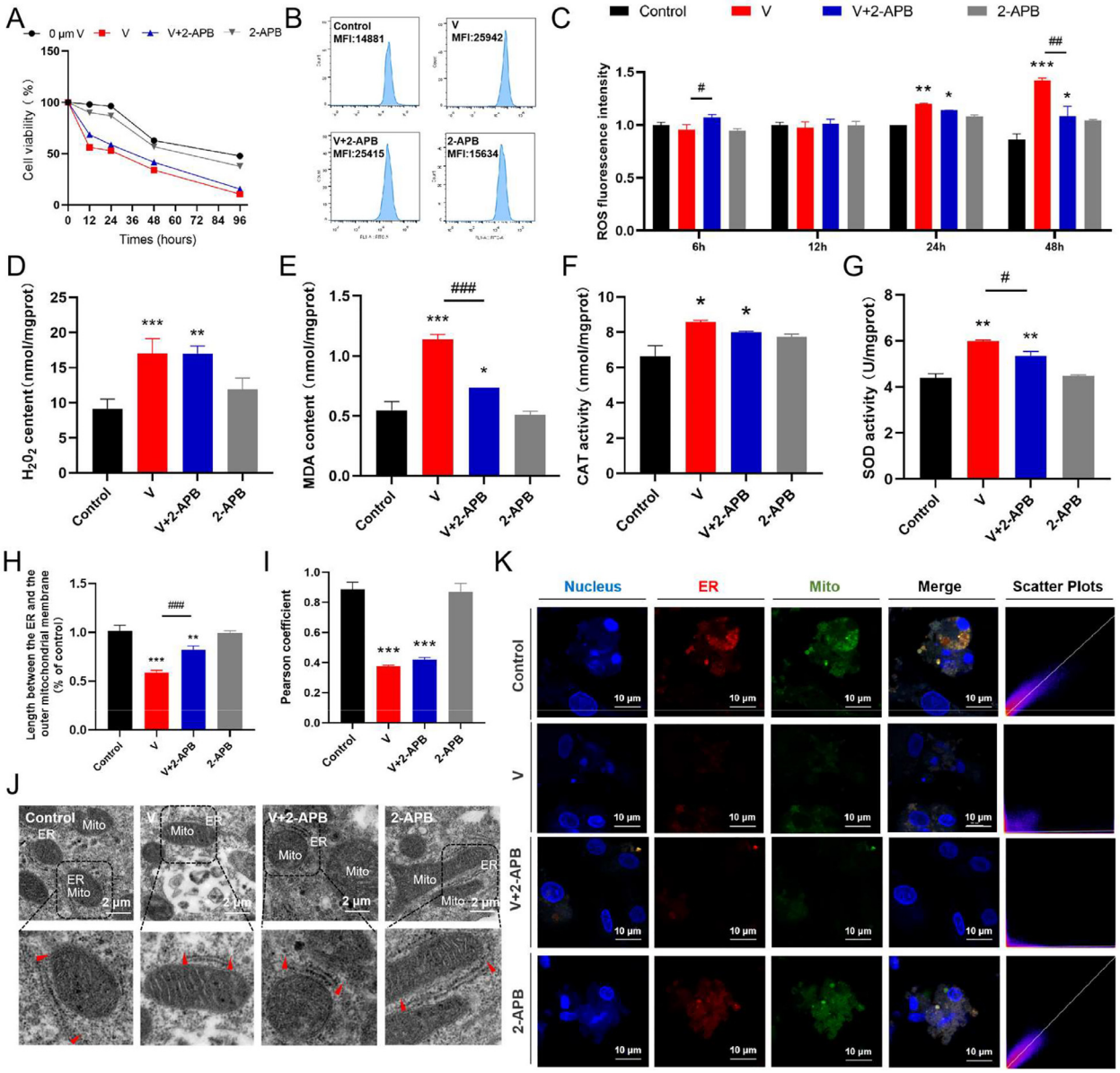

Figure 4. 2-APB alleviated V exposure-induced duck hepatocyte injury and MAM structural abnormalities. (A) Changes in cell viability at 12, 24, 48, and 96 h structural abnormalities. (B) ROS production at 24 h. (C) ROS levels at 6, 12, 24, and 48 h. (D–G) Oxidative stress indices. (H) Analysis of MAM length. (I) Pearson's coefficient analysis correlation of ER and Mito staining. (J) Ultrastructural observation. Mito: mitochondria; red arrows: ER-mitochondria coupling. (K) LSCM detection of ER and mitochondrial interactions (*$P < 0.05$ vs. Control, **$P < 0.01$ vs. Control, ***$P < 0.001$ vs. Control; #$P < 0.05$ vs. V, ##$P < 0.01$ vs. V; ###$P < 0.001$ vs. V).

intensity of NLRP3 and ASC was reduced under V treatment. The cotreatment of 2-APB moderated those variations caused by V ($P < 0.01$ or $P < 0.001$).

The mRNA levels of NLRP3, ASC, IL-18, and IL-1β were significantly decreased after V+2-APB treatment compared with the V group ($P < 0.01$ or $P < 0.001$) (Figure 6E and F). Compared with those in the V group, the NLRP3, ASC, and caspase-1 protein levels in the 2-APB group were also significantly decreased (Figure 6G and H) ($P < 0.001$).

DISCUSSION

The performance of V in the immune system is very apparent, as this element has a potentially detrimental influence on different kinds of organs (Hanus-Fajerska et al., 2021). Generally, the toxicity of V is involves disturbing Ca^{2+} channels, along with multisystem and autoimmune disorders (Bhuvaneshwari and Sankaranarayanan, 2020). Research has shown that V exposure can disrupt the function of mitochondria and ER and promote the hepatocyte death by leading to MAMs dysfunction (Hu et al., 2021; Xiong et al., 2021). Furthermore, the mechanisms of inflammation induction by calcium homeostasis disorder have been extensively studied. Therefore, the interaction between MAMs dysfunction and inflammation induced by V through calcium homeostasis deserves further investigation. Hence, this study aimed to investigate the V-induced toxic events occurring in duck hepatocytes, focusing on the mechanism of MAMs and intracellular inflammation.

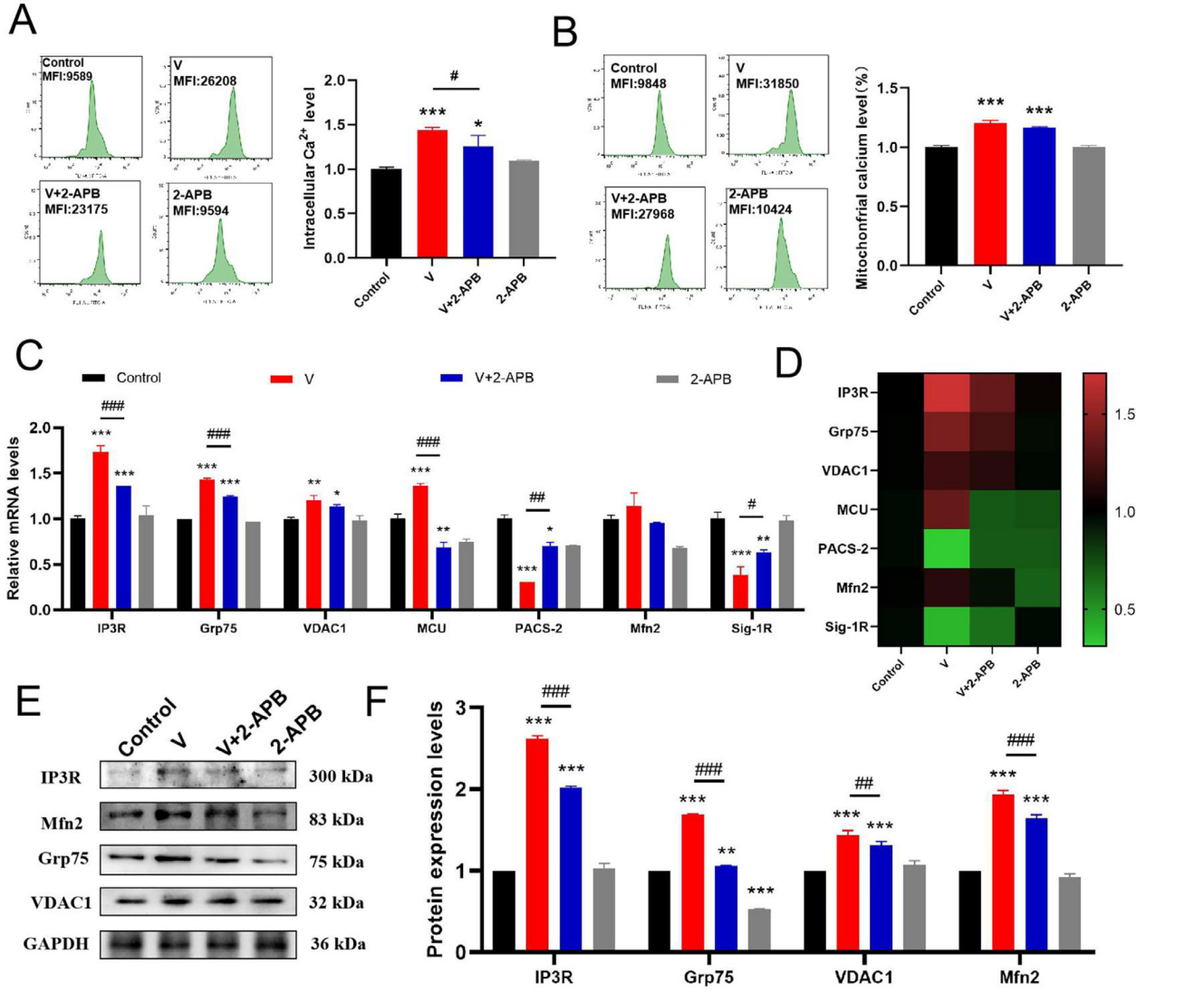

Figure 5. 2-APB regulated V-induced MAM dysfunction-related mRNA and protein levels by regulating calcium homeostasis. (A) Intracellular Ca^{2+} level. (B) Mitochondrial Ca^{2+} level. (C and D) mRNA levels of MAM-related factors. (E and F) Protein levels of MAM-related factors. ($^{*}P < 0.05$ vs. Control, $^{**}P < 0.01$ vs. Control, $^{***}P < 0.001$ vs. Control; $\#P < 0.05$ vs. V, $\#\#P < 0.01$ vs. V; $\#\#\#P < 0.001$ vs. V).

Based on culturing primary duck hepatocytes, the effects of V on MAMs dynamics and inflammation and the molecular crosstalk between MAMs coupling and inflammation were explored.

A previously study reported that the pathological changes and ultrastructural pathology of hepatocytes are induced under V exposure (Cervantes-Valencia et al., 2021). V exposure decreased cell viability and destroyed nuclear DNA (**nDNA**) and mitochondrial DNA (**mtDNA**), resulting in mitochondrial damage and dysfunction (Rivas-Garcia et al., 2020; Wang et al., 2023). Our results showed that V exposure-induced vacuolization of hepatocytes, decreased the cell density and enlarged the intercellular space with decreasing cell viability. Moreover, enhanced production of ROS and oxidative stress occurred in mitochondria and ER on account of V exposure, resulting in inflammation (Jomova and Valko, 2011; Burgos-Moron et al., 2019). MDA, SOD, CAT, and H_2O_2 are recognized as important biomarkers of oxidative stress. The generation of SOD and CAT can alleviate the oxidative stress caused by ROS (Liu et al., 2021; Aziz et al., 2022). Simultaneously, SOD converts superoxide O^{2-} generated by oxidative stress into H_2O_2, and then CAT decomposes H_2O_2 into water and oxygen (Wang et al., 2018; Yang et al., 2019). MDA, an indispensable component of oxidative stress, represents the degree of cell membrane system damage and can also exacerbate damage to the cell membrane (Aziz et al., 2021; Shi et al., 2021). Our findings showed that the level of cellular ROS was aggravated under the induction of V, and the production of antioxidants also confirmed that V caused cellular oxidative stress in duck hepatocytes.

The accumulation of high levels of ROS could lead to structural and functional alterations in MAMs (Aziz et al., 2021; Resende et al., 2022). Several study researches have indicated that heavy metals can cause oxidative stress and MAMs structural abnormalities in different cells (Li et al., 2018; Che et al., 2021; Paithankar et al., 2021). Similarly, our study showed that the membrane surface area and length of MAMs decreased under the stress of V, which implied damage to MAMs. Defects in MAMs have multidirectional effects on a wide

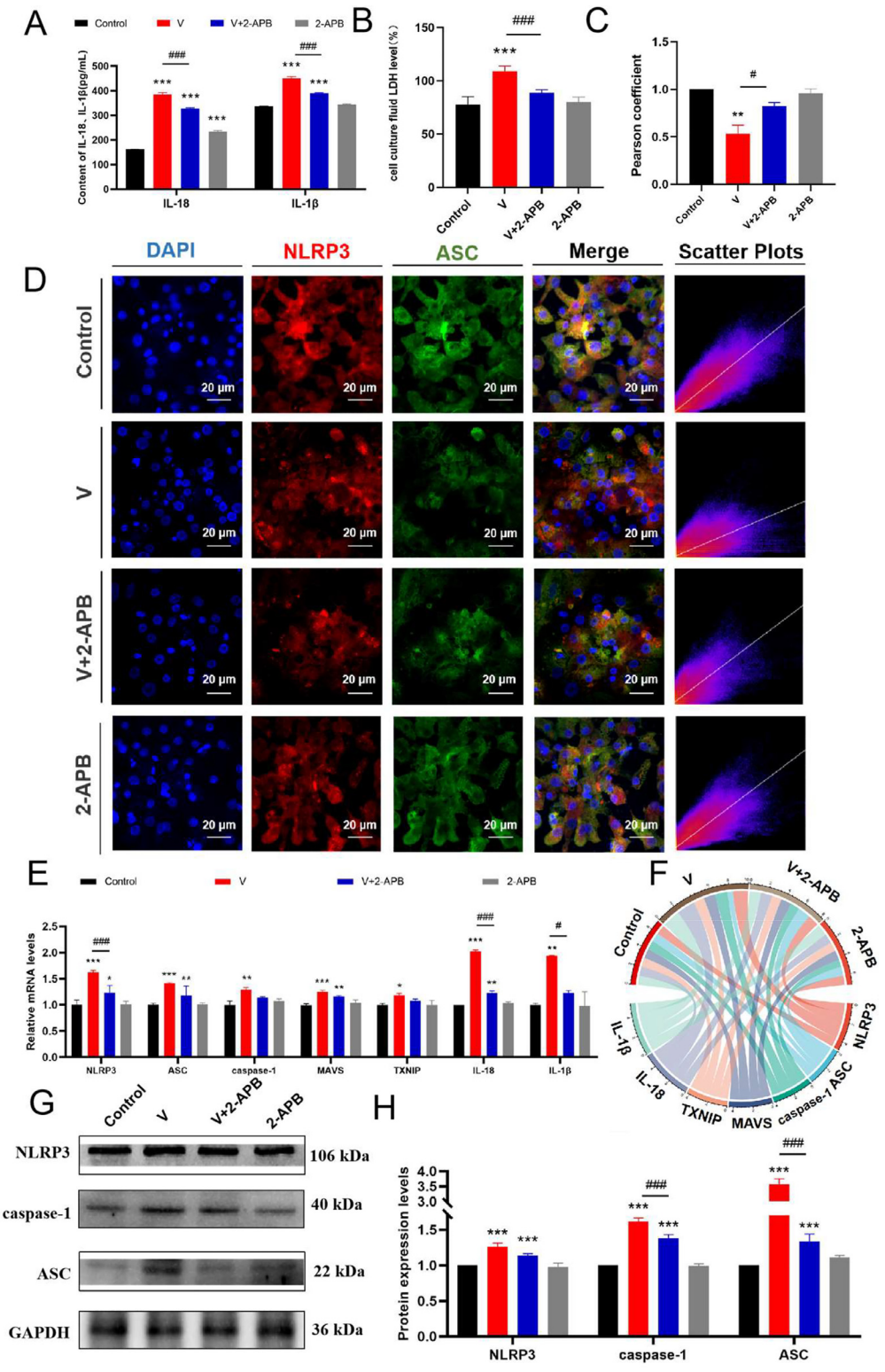

Figure 6. 2-APB alleviated V-induced duck hepatocyte inflammation. (A) IL-18 and IL-1β activities in the cell supernatant. (B) LDH activity in the cell supernatant. (C) The Pearson correlation coefficient of the colocalization of NLRP3 and ASC. (D) Observation of the colocalization of NLRP3 and ASC. (E and F) mRNA levels of inflammation-related factors. (G and H) Protein levels of inflammation-related factors (*$P < 0.05$ vs. Control, **$P < 0.01$ vs. Control, ***$P < 0.001$ vs. Control; #$P < 0.05$ vs. V, ##$P < 0.01$ vs. V; ###$P < 0.001$ vs. V).

range of intracellular activities, leading to Ca^{2+} dyshomeostasis and inflammasome activation, which all contribute to the onset and progression of liver diseases (Gao et al., 2020). Consequently, our findings suggested that V exposure-induced duck hepatocyte injury and MAMs dysfunction by triggering pathological changes, ultrastructural pathology, and intracellular oxidative stress.

MAMs constitute the physical connection and powerful functional complex between the ER and mitochondria but also ensure the normal function of the Ca^{2+} signaling pathway between them (Hamilton et al., 2020;

Zhao et al., 2021). Abnormal MAMs structure can lead to continuous Ca^{2+} transfer from the ER to mitochondria, causing mitochondrial Ca^{2+} overload and mitochondrial dysfunction (Zhang et al., 2021). Alteration of MAMs and cellular components by Ca^{2+} disorder affects cellular mechanisms such as autophagy or inflammation (Burgos-Moron et al., 2019; Zhang et al., 2021). It was determined that an imbalance in Ca^{2+} homeostasis led to IP_3R expression level upregulation (Ye et al., 2021). Our results indicated that Ca^{2+} transfer was excessive and persistently induced by V exposure. IP_3R, VDAC1, Grp75, Mfn2, PACS-2, MCU, and Sig-1R are the key regulatory factors that regulate the mechanism of calcium signaling. Evidence suggests that the macromolecular complex formed by IP_3R, Grp75, and VDAC1 mediates the transport of Ca^{2+} from the ER to mitochondria. Ca^{2+} released from the ER enters the mitochondrial matrix through MCU (mitochondrial calcium single transporter) (Xu et al., 2018). Sig-1R interacts with IP_3R and maintains Ca^{2+} signal transduction from the ER to mitochondria (Fan and Simmen, 2019). MFN2 and PACS-2, as the connecting proteins through MAMs, promote the integrity of MAMs and regulate their composition (Myhill et al., 2008). Previous studies have shown that ER-mitochondria contact sites were reduced through the impairment of the GRP75-IP_3R interaction in dysfunctional cells caused by V, suggesting a deregulation in MAMs activity (Erustes et al., 2021). Similarly, our findings revealed that V exposure upregulated the mRNA levels of MAMs-related factors (IP_3R, VDAC1, Grp75, Mfn2, and MCU) and the protein levels of MAMs-related factors (IP_3R, VDAC1, Grp75, and Mfn2), resulting in MAMs disorder in hepatocytes. Calcium homeostasis imbalance induces changes in cellular composition leading to structural disruption of MAMs, resulting in autophagy or inflammation (Burgos-Moron et al., 2019). Above all, the findings suggested that V might induce MAMs dysfunction by triggering Ca^{2+} disorder in hepatocytes.

MAMs have been proven to offer a molecular platform for NLRP3 inflammasome formation to play a pivotal role in inflammatory reactions (Missiroli et al., 2018). Oligomerized NLRP3 recruits ASC via homotypic pyrin domain (**PYD**) interactions and induces the aggregation of ASC into a macromolecular focus. Subsequently, the assembled ASC recruits procaspase-1 to form the NLRP3-ASC-caspase-1 protein complex, which is called the NLRP3 inflammasome (Huang et al., 2021). Meanwhile, pro-IL-1β and pro-IL-18, generated from the prestimulation signal in the activation signal, were sheared to produce mature and active inflammatory factors, exerting the proinflammatory role with the NLRP3 inflammasome (Wang et al., 2021). Generally, inflammation is a multifaceted process involving numerous molecular and cellular mechanisms between the pathogen and the host, which is often correlated with MAMs dysfunction, calcium homeostasis regulation and ROS (Pereira et al., 2022). Inflammation is regulated by the markers of the inflammation-related activation complex (NLRP3, ASC, and caspase-1), the product of inflammation (IL-18, IL-1β), mitochondrial antiviral signal protein (MAVS) and thioredoxin-interacting protein (TXNIP). A previous study showed that Cd could increase ROS production and activate NLRP3, thereby enhancing the secretion of IL-18 and IL-1β (Li et al., 2021). Likewise, our results indicated a large amount of IL-18 and IL-1β in the supernatants, which was consistent with previous studies. Similarly, our findings indicated that V exposure-induced inflammation by upregulating inflammation-related mRNA factors (NLRP3, ASC, caspase-1, MAVS, TXNIP IL-18, and IL-1β) and inflammation-related protein factors (NLRP3, ASC, caspase-1), which indicated the occurrence of inflammation in hepatocytes. Generally, our results demonstrated that V could trigger MAMs disorders by disrupting calcium homeostasis, resulting in inflammation in hepatocytes.

MAMs contact sites provide a site for activation of NLRP3, which not only accelerates the storage of Ca^{2+} from the ER to mitochondria, but also increases Ca^{2+} in the cytoplasm to promote the assembly of inflammatory components and control key mitochondrial functions (Xu et al., 2020; Zhai et al., 2022). They provide important substances and sites for the activation of the inflammatory response, and Ca^{2+} plays a key role in MAMs and inflammatory mechanisms. IP_3R is the most ubiquitous intracellular Ca^{2+} channel, and inhibition of IP_3R can slow the release of Ca^{2+} from the ER into the cytosol and mitochondria, which can alleviate MAMs disorder to a certain extent (Paknejad and Hite, 2018). To explore the relationship between MAMs dysfunction and inflammation, we used 2-APB as an IP_3R blocker to inhibit the Ca^{2+} transport channel. Liang et al. (2018) reported that hepatocytes cultured with 2-APB inhibited Ca^{2+} from entering cells and alleviated the disturbance of Ca^{2+} transport. Our results revealed that an IP_3R inhibitor attenuated V-induced Ca^{2+} disorder and MAMs morphological damage, and upregulated MAMs-related gene (Mfn2, Grp75, IP_3R, VDAC1, MCU) and protein levels (Mfn2, Grp75, VDAC1, IP_3R). Similarly, we found that an IP_3R inhibitor could reduce LDH, IL-18, and IL-1β activity in the cell supernatant, alleviate the degree of cell membrane damage, and reduce the increase in intracellular and intramitochondrial Ca^{2+} concentrations under V exposure. In addition, inhibition of IP_3R attenuated V-induced upregulation of inflammation-related factors. These results indicated that relieving MAMs dysfunction could attenuate V-induced cellular inflammation. Therefore, our findings further suggested that alleviating MAMs dysfunction by inhibiting IP_3R could ameliorate V-induced inflammation.

CONCLUSIONS

The results revealed that excessive V could lead to the disruption of the structure and function of MAMs as well as the destruction of cell calcium homeostasis and inflammation in duck hepatocytes. However, relieving MAMs dysfunction could reduce V-induced inflammation.

DISCLOSURES

The authors declare that they have no known competing financial interests or personal relationships that could have appeared to influence the work reported in the present study.

ACKNOWLEDGMENTS

This research was funded by the National Natural Science Foundation of China (No. 31902333), Jiangxi Provincial Natural Science Foundation (20212BAB215017) and Science and Technology Plan of Education Department of Jiangxi Province (GJJ190216).

SUPPLEMENTARY MATERIALS

Supplementary material associated with this article can be found in the online version at doi:10.1016/j.psj.2023.103013.

REFERENCES

Adebiyi, O. E., J. O. Olopade, and F. O. Olayemi. 2018. Sodium metavanadate induced cognitive decline, behavioral impairments, oxidative stress and down regulation of myelin basic protein in mice hippocampus: ameliorative roles of beta-spinasterol, and stigmasterol. Brain Behav. 8:e1014.

Ahumada-Castro, U., G. Bustos, E. Silva-Pavez, A. Puebla-Huerta, A. Lovy, and C. Cardenas. 2021. In the right place at the right time: regulation of cell metabolism by iP3R-mediated inter-organelle Ca(2+) fluxes. Front Cell Dev. Biol. 9:629522.

Aziz, S., S. Abdullah, H. Anwar, and F. Latif. 2022. DNA damage and oxidative stress in economically important fish, bighead carp (hypophthalmichthys nobilis) exposed to engineered copper oxide nanoparticles. Pak. Vet. J. 42:1–8.

Aziz, S., S. Abdullah, H. Anwar, F. Latif, and W. Mustfa. 2021. Effect of engineered nickel oxide nanoparticles on antioxidant enzymes in freshwater fish, Labeo rohita. Pak. Vet. J. 41:424–428.

Bai, H., F. Yang, W. Jiang, A. Hu, H. Chang, Y. Zhang, L. Jiang, S. Lin, Z. Lu, C. Zhang, and H. Cao. 2021. Molybdenum and cadmium co-induce mitophagy and mitochondrial dysfunction via ROS-mediated PINK1/Parkin pathway in Hepa1-6 cells. Ecotoxicol. Environ. Saf. 224:112618.

Bai, B., Y. Yang, Q. Wang, M. Li, C. Tian, Y. Liu, L. Aung, P. F. Li, T. Yu, and X. M. Chu. 2020. NLRP3 inflammasome in endothelial dysfunction. Cell Death Dis. 11:776.

Barazzuol, L., F. Giamogante, and T. Cali. 2021. Mitochondria associated membranes (MAMs): architecture and physiopathological role. Cell Calcium 94:102343.

Bhuvaneshwari, S., and K. Sankaranarayanan. 2020. Structural and mechanistic insights of CRAC channel as a drug target in autoimmune disorder. Curr. Drug Targets 21:55–75.

Burgos-Moron, E., Z. Abad-Jimenez, A. M. Maranon, F. Iannantuoni, I. Escribano-Lopez, S. Lopez-Domenech, C. Salom, A. Jover, V. Mora, I. Roldan, E. Sola, M. Rocha, and V. M. Victor. 2019. Relationship vetween oxidative stress, ER stress, and inflammation in type 2 diabetes: the battle continues. J. Clin. Med. 8:1385.

Cervantes-Valencia, M. E., A. Gonzalez-Villalva, G. Cano-Gutierrez, J. C. Albarran-Alonso, and T. I. Fortoul. 2021. Effects of vanadium inhalation and sweetened beverage ingestion in mice: morphological and biochemical changes in the liver. Int. J. Toxicol. 40:466–474.

Che, L., C. L. Yang, Y. Chen, Z. L. Wu, Z. B. Du, J. S. Wu, C. L. Gan, S. P. Yan, J. Huang, N. J. Guo, Y. C. Lin, and Z. N. Lin. 2021. Mitochondrial redox-driven mitofusin 2 S-glutathionylation promotes neuronal necroptosis via disrupting ER-mitochondria crosstalk in cadmium-induced neurotoxicity. Chemosphere 262:127878.

Chetelat, J., S. G. Nielsen, M. Auro, D. Carpenter, L. Mundy, and P. J. Thomas. 2021. Vanadium stable isotopes in biota of terrestrial and aquatic food chains. Environ. Sci. Technol. 55:4813–4821.

Dai, X. Y., X. W. Li, S. Y. Zhu, M. Z. Li, Y. Zhao, M. Talukder, Y. H. Li, and J. L. Li. 2021. Lycopene ameliorates di(2-ethylhexyl) phthalate-induced pyroptosis in spleen via suppression of classic caspase-1/NLRP3 pathway. J. Agric. Food Chem. 69:1291–1299.

Dai, X. Y., S. Y. Zhu, J. Chen, M. Z. Li, Y. Zhao, M. Talukder, and J. L. Li. 2022. Lycopene alleviates di(2-ethylhexyl) phthalate-induced splenic injury by activating P62-Keap1-NRF2 signaling. Food Chem. Toxicol. 168:113324.

Delfert, D. M., and J. M. McDonald. 1985. Vanadyl and vanadate inhibit Ca^{2+} transport systems of the adipocyte plasma membrane and endoplasmic reticulum. Arch. Biochem. Biophys. 241:665–672.

Ea, M., M. El-Attrouny, S. Baloza, and S. Ramadan. 2022. Selection for high body weight and its association with the expression profiles of somatotropic axis and mitochondrial genes in japanese quail. Pakistan Vet. J. 42:261–265.

Erustes, A. G., M. D'Eletto, G. C. Guarache, R. P. Ureshino, C. Bincoletto, S. P. G. Da, M. Piacentini, and S. S. Smaili. 2021. Overexpression of alpha-synuclein inhibits mitochondrial Ca(2+) trafficking between the endoplasmic reticulum and mitochondria through MAMs by altering the GRP75-IP3R interaction. J. Neurosci. Res. 99:2932–2947.

Fan, Y., and T. Simmen. 2019. Mechanistic connections between endoplasmic reticulum (ER) redox control and mitochondrial metabolism. Cells-Basel 8:1071.

Fang, Y., C. Xing, X. Wang, H. Cao, C. Zhang, X. Guo, Y. Zhuang, R. Hu, G. Hu, and F. Yang. 2021. Activation of the ROS/HO-1/NQO1 signaling pathway contributes to the copper-induced oxidative stress and autophagy in duck renal tubular epithelial cells. Sci. Total Environ. 757:143753.

Gao, P., W. Yang, and L. Sun. 2020. Mitochondria-associated endoplasmic reticulum membranes (MAMs) and their prospective roles in kidney disease. Oxid. Med. Cell Longev. 2020:3120539.

Hamilton, S., R. Terentyeva, B. Martin, F. Perger, J. Li, A. Stepanov, I. M. Bonilla, B. C. Knollmann, P. B. Radwanski, S. Gyorke, A. E. Belevych, and D. Terentyev. 2020. Increased RyR2 activity is exacerbated by calcium leak-induced mitochondrial ROS. Basic Res. Cardiol. 115:38.

Han, X., T. Xu, Q. Fang, H. Zhang, L. Yue, G. Hu, and L. Sun. 2021. Quercetin hinders microglial activation to alleviate neurotoxicity via the interplay between NLRP3 inflammasome and mitophagy. Redox Biol. 44:102010.

Hanus-Fajerska, E., A. Wiszniewska, and I. Kaminska. 2021. A dual role of vanadium in environmental systems - beneficial and detrimental effects on terrestrial plants and humans. Plants (Basel) 10:1110.

Harland, B. F., and B. A. Harden-Williams. 1994. Is vanadium of human nutritional importance yet? J. Am. Diet. Assoc. 94:891–894.

Hosseini, M. J., F. Shaki, M. Ghazi-Khansari, and J. Pourahmad. 2013. Toxicity of vanadium on isolated rat liver mitochondria: a new mechanistic approach. Metallomics 5:152–166.

Hu, D., H. Xu, W. Zhang, X. Xu, B. Xiao, X. Shi, Z. Zhou, N. Slater, Y. Shen, and J. Tang. 2021. Vanadyl nanocomplexes enhance photothermia-induced cancer immunotherapy to inhibit tumor metastasis and recurrence. Biomaterials 277:121130.

Huang, Y., W. Xu, and R. Zhou. 2021. NLRP3 inflammasome activation and cell death. Cell. Mol. Immunol. 18:2114–2127.

Janka, Z. 2019. Tracing trace elements in mental functions. Ideggyogy Sz. 72:367–379.

Jomova, K., and M. Valko. 2011. Advances in metal-induced oxidative stress and human disease. Toxicology 283:65–87.

Krols, M., G. van Isterdael, B. Asselbergh, A. Kremer, S. Lippens, V. Timmerman, and S. Janssens. 2016. Mitochondria-associated membranes as hubs for neurodegeneration. Acta Neuropathol. 131:505–523.

Li, W., T. Cao, C. Luo, J. Cai, X. Zhou, X. Xiao, and S. Liu. 2020. Crosstalk between ER stress, NLRP3 inflammasome, and inflammation. Appl. Microbiol. Biotechnol. 104:6129–6140.

Li, Z., H. Chi, W. Zhu, G. Yang, J. Song, L. Mo, Y. Zhang, Y. Deng, F. Xu, J. Yang, Z. He, and X. Yang. 2021. Cadmium induces renal inflammation by activating the NLRP3 inflammasome through

ROS/MAPK/NF-kappaB pathway in vitro and in vivo. Arch. Toxicol. 95:3497–3513.
Li, L., J. Cui, Z. Liu, X. Zhou, Z. Li, Y. Yu, Y. Jia, D. Zuo, and Y. Wu. 2018. Silver nanoparticles induce SH-SY5Y cell apoptosis via endoplasmic reticulum- and mitochondrial pathways that lengthen endoplasmic reticulum-mitochondria contact sites and alter inositol-3-phosphate receptor function. Toxicol. Lett. 285:156–167.
Liang, Q., Y. Zhang, M. Zeng, L. Guan, Y. Xiao, and F. Xiao. 2018. The role of IP3R-SOCCs in Cr(vi)-induced cytosolic Ca(2+) overload and apoptosis in L-02 hepatocytes. Toxicol. Res. (Camb). 7:521–528.
Lin, S., F. Yang, M. Hu, J. Chen, G. Chen, A. Hu, X. Li, D. Fu, C. Xing, Z. Xiong, Y. Wu, and H. Cao. 2023. Selenium alleviates cadmium-induced mitophagy through FUNDC1-mediated mitochondrial quality control pathway in the lungs of sheep. Environ. Pollut. 319:120954.
Liu, B. X., Y. Li, M. Khalid, N. Fazul, A. T. Shakeel, F. Mehwish, M. Ashraf, Z. Tang, and H. Zhang. 2021. Role of oxidative stress and antioxidants in thiram-induced tibial dyschondroplasia. Pak. Vet. J. 41:1–6.
Marchi, S., M. Bittremieux, S. Missiroli, C. Morganti, S. Patergnani, L. Sbano, A. Rimessi, M. Kerkhofs, J. B. Parys, G. Bultynck, C. Giorgi, and P. Pinton. 2017. Endoplasmic reticulum-mitochondria communication through Ca(2+) signaling: the importance of mitochondria-associated membranes (MAMs). Adv. Exp. Med. Biol. 997:49–67.
Miao, Z., Z. Miao, S. Wang, H. Wu, and S. Xu. 2022a. Exposure to imidacloprid induce oxidative stress, mitochondrial dysfunction, inflammation, apoptosis and mitophagy via NF-kappaB/JNK pathway in grass carp hepatocytes. Fish Shellfish Immunol. 120:674–685.
Missiroli, S., S. Patergnani, N. Caroccia, G. Pedriali, M. Perrone, M. Previati, M. R. Wieckowski, and C. Giorgi. 2018. Mitochondria-associated membranes (MAMs) and inflammation. Cell Death Dis. 9:329.
Montesinos, J., and E. Area-Gomez. 2020. Isolation of mitochondria-associated ER membranes. Methods Cell. Biol. 155:33–44.
Myhill, N., E. M. Lynes, J. A. Nanji, A. D. Blagoveshchenskaya, H. Fei, S. K. Carmine, T. J. Cooper, G. Thomas, and T. Simmen. 2008. The subcellular distribution of calnexin is mediated by PACS-2. Mol. Biol. Cell 19:2777–2788.
Paithankar, J. G., S. Saini, S. Dwivedi, A. Sharma, and D. K. Chowdhuri. 2021. Heavy metal associated health hazards: An interplay of oxidative stress and signal transduction. Chemosphere 262:128350.
Paknejad, N., and R. K. Hite. 2018. Structural basis for the regulation of inositol trisphosphate receptors by Ca(2+) and IP(3). Nat. Struct. Mol. Biol. 25:660–668.
Panchal, S. K., S. Wanyonyi, and L. Brown. 2017. Selenium, vanadium, and chromium as micronutrients to improve metabolic syndrome. Curr. Hypertens. Rep. 19:10.
Park, Y. J., S. A. Yoo, M. Kim, and W. U. Kim. 2020. The role of calcium-calcineurin-NFAT signaling pathway in health and autoimmune diseases. Front. Immunol. 11:195.
Peng, J., C. Peng, L. Wang, H. Cao, C. Xing, G. Li, G. Hu, and F. Yang. 2022. Endoplasmic reticulum-mitochondria coupling attenuates vanadium-induced apoptosis via IP3R in duck renal tubular epithelial cells. J. Inorg. Biochem. 232:111809.
Pereira, A. C., J. De Pascale, R. Resende, S. Cardoso, I. Ferreira, B. M. Neves, M. A. Carrascal, M. Zuzarte, N. Madeira, S. Morais, A. Macedo, C. A. Do, P. I. Moreira, M. T. Cruz, and C. F. Pereira. 2022. ER-mitochondria communication is involved in NLRP3 inflammasome activation under stress conditions in the innate immune system. Cell. Mol. Life. Sci. 79:213.
Renu, K., R. Chakraborty, H. Myakala, R. Koti, A. C. Famurewa, H. Madhyastha, B. Vellingiri, A. George, and G. A. Valsala. 2021. Molecular mechanism of heavy metals (lead, chromium, arsenic, mercury, nickel and cadmium) - induced hepatotoxicity - a review. Chemosphere 271:129735.
Resende, R., T. Fernandes, A. C. Pereira, A. P. Marques, and C. F. Pereira. 2022. ER-mitochondria contacts modulate ROS-mediated signaling and oxidative stress in brain disorders: the key role of Sigma-1 receptor. Antioxid. Redox Signal. 37:758–780.
Rivas-Garcia, L., J. L. Quiles, A. Varela-Lopez, M. Arredondo, P. Lopez, A. R. Dieguez, M. Montes-Bayon, P. Aranda, J. Llopis, and C. Sanchez-Gonzalez. 2020. In vitro study of the protective effect of manganese against vanadium-mediated nuclear and mitochondrial DNA damage. Food Chem. Toxicol. 135:110900.
Scibior, A., L. Pietrzyk, Z. Plewa, and A. Skiba. 2020. Vanadium: risks and possible benefits in the light of a comprehensive overview of its pharmacotoxicological mechanisms and multi-applications with a summary of further research trends. J. Trace Elem. Med. Biol. 61:126508.
Shi, W., J. Lou, X. Zhang, Y. Ji, X. Weng, and J. Du. 2021. Adipose tissue alleviates the stress response by releasing adiponectin during laparoscopic surgery in patients with colorectal cancer. Lipids Health Dis. 20:166.
Slominski, A. 1991. POMC gene expression in mouse and hamster melanoma cells. FEBS Lett. 291:165–168.
Song, X. B., G. Liu, F. Liu, Z. G. Yan, Z. Y. Wang, Z. P. Liu, and L. Wang. 2017. Autophagy blockade and lysosomal membrane permeabilization contribute to lead-induced nephrotoxicity in primary rat proximal tubular cells. Cell Death Dis. 8:e2863.
Tripathi, D., V. Mani, and R. P. Pal. 2018. Vanadium in biosphere and its role in biological processes. Biol. Trace Elem. Res. 186:52–67.
Wang, Y., R. Branicky, A. Noe, and S. Hekimi. 2018. Superoxide dismutases: dual roles in controlling ROS damage and regulating ROS signaling. J. Cell Biol. 217:1915–1928.
Wang, L., Y. Pan, F. Yang, X. Guo, J. Peng, X. Wang, Y. Fang, J. Chen, X. Yi, H. Cao, and G. Hu. 2022a. New sight into interaction between endoplasmic reticulum stress and autophagy induced by vanadium in duck renal tubule epithelial cells. Chem. Biol. Interact. 362:109981.
Wang, X., C. Xing, G. Li, X. Dai, X. Gao, Y. Zhuang, H. Cao, G. Hu, X. Guo, and F. Yang. 2023. The key role of proteostasis at mitochondria-associated endoplasmic reticulum membrane in vanadium-induced nephrotoxicity using a proteomic strategy. Sci. Total Environ. 869:161741.
Wang, C., T. Yang, J. Xiao, C. Xu, Y. Alippe, K. Sun, T. D. Kanneganti, J. B. Monahan, Y. Abu-Amer, J. Lieberman, and G. Mbalaviele. 2021. NLRP3 inflammasome activation triggers gasdermin D-independent inflammation. Sci. Immunol. 6: j3859.
Wang, Z., S. Zhang, Y. Xiao, W. Zhang, S. Wu, T. Qin, Y. Yue, W. Qian, and L. Li. 2020. NLRP3 inflammasome and inflammatory diseases. Oxid. Med. Cell. Longev. 2020:4063562.
Widowati, W., S. Prahastuti, M. Hidayat, S. T. Hasiana, R. Wahyudianingsih, E. Afifah, HSW. Kusuma, R. Rizal, and M. Subangkit. 2022. Protective effect of ethanolic extract of Jati Belanda (Guazuma ulmifolia L.) by inhibiting oxidative stress and inflammatory processes in cisplatin-induced nephrotoxicity in rats. Pak. Vet. J. 42:376–382.
Xiong, Z., C. Xing, T. Xu, Y. Yang, G. Liu, G. Hu, H. Cao, C. Zhang, X. Guo, and F. Yang. 2021. Vanadium induces oxidative stress and mitochondrial quality control disorder in the heart of ducks. Front. Vet. Sci. 8:756534.
Xu, H., N. Guan, Y. L. Ren, Q. J. Wei, Y. H. Tao, G. S. Yang, X. Y. Liu, D. F. Bu, Y. Zhang, and S. N. Zhu. 2018. IP3R-Grp75-VDAC1-MCU calcium regulation axis antagonists protect podocytes from apoptosis and decrease proteinuria in an adriamycin nephropathy rat model. BMC Nephrol. 19:140.
Xu, F., H. Qi, J. Li, L. Sun, J. Gong, Y. Chen, A. Shen, and W. Li. 2020. Mycobacterium tuberculosis infection up-regulates MFN2 expression to promote NLRP3 inflammasome formation. J. Biol. Chem. 295:17684–17697.
Xu, S., L. Xiaojing, S. Xinyue, C. Wei, L. Honggui, and X. Shiwen. 2021. Pig lung fibrosis is active in the subacute $CdCl_2$ exposure model and exerts cumulative toxicity through the M1/M2 imbalance. Ecotoxicol. Environ. Saf. 225:112757.
Yang, M., C. Li, S. Yang, Y. Xiao, X. Xiong, W. Chen, H. Zhao, Q. Zhang, Y. Han, and L. Sun. 2020. Mitochondria-associated ER membranes - the origin site of autophagy. Front. Cell Dev. Biol. 8:595.
Yang, F., J. Liao, R. Pei, W. Yu, Q. Han, Y. Li, J. Guo, L. Hu, J. Pan, and Z. Tang. 2018. Autophagy attenuates copper-induced mitochondrial dysfunction by regulating oxidative stress in chicken hepatocytes. Chemosphere 204:36–43.

Yang, F., R. Pei, Z. Zhang, J. Liao, W. Yu, N. Qiao, Q. Han, Y. Li, L. Hu, J. Guo, J. Pan, and Z. Tang. 2019. Copper induces oxidative stress and apoptosis through mitochondria-mediated pathway in chicken hepatocytes. Toxicol. In Vitro 54:310–316.

Ye, L., Q. Zeng, M. Ling, R. Ma, H. Chen, F. Lin, Z. Li, and L. Pan. 2021. Inhibition of IP3R/Ca^{2+} dysregulation protects mice from ventilator-induced lung injury via endoplasmic reticulum and mitochondrial pathways. Front. Immunol. 12:729094.

Yuan, Z. H., K. Y. Zhang, X. M. Ding, Y. H. Luo, S. P. Bai, Q. F. Zeng, and J. P. Wang. 2016. Effect of tea polyphenols on production performance, egg quality, and hepatic antioxidant status of laying hens in vanadium-containing diets. Poult. Sci. 95:1709–1717.

Zhai, Q., X. Chen, D. Fei, X. Guo, X. He, W. Zhao, S. Shi, J. J. Gooding, F. Jin, Y. Jin, and B. Li. 2022. Nanorepairers rescue inflammation-induced mitochondrial dysfunction in mesenchymal stem cells. Adv. Sci. (Weinh). 9:e2103839.

Zhang, C., T. Lin, G. Nie, R. Hu, S. Pi, Z. Wei, C. Wang, G. Li, and G. Hu. 2021. In vivo assessment of molybdenum and cadmium co-induce nephrotoxicity via causing calcium homeostasis disorder and autophagy in ducks (Anas platyrhyncha). Ecotoxicol. Environ. Saf. 230:113099.

Zhao, Y., J. G. Cui, H. Zhang, X. N. Li, M. Z. Li, M. Talukder, and J. L. Li. 2021. Role of mitochondria-endoplasmic reticulum coupling in lycopene preventing DEHP-induced hepatotoxicity. Food Funct. 12:10741–10749.

Zhou, Y., L. Gao, D. Xu, and B. Gao. 2019. Geochemical baseline establishment, environmental impact and health risk assessment of vanadium in lake sediments, China. Sci. Total. Environ. 660:1338–1345.